E-/H-mode transition of inductively coupled oxygen RF discharges

Th. Wegner, C. Küllig, J. Meichsner

Institute of Physics, University of Greifswald, Germany

Introduction

Inductively coupled radio frequency discharges (ICP) are relevant for plasma echting, surface treatment and functionalization and especially for the sterilization and decontamination of sensitive surfaces. The electrodeless discharge arrangement leads to higher densities at lower pressures and reduced ion energy due to lower plasma sheath potential. Due to higher plasma density the collision rates will by enforced, e.g., for dissociation and chemical reactions in molecule plasmas, excitation and ionization.

A planar oxygen discharge driven at 13.56 MHz was investigated in detail by comprehensive plasma diagnostics which are described in the next section. Especially, the Langmuir probe measurement, the 160 GHz Gaussian beam microwave interferometry, the optical emission and VUV absorption spectroscopy were used to study the mode transition from the capacitive (E-) to the inductive (H-) mode [1] of an oxygen ICP. To control the mode transition the coil voltage (peak-to-peak-voltage) was chosen as an applicable process parameter. The mode transition is characterized by the decrease of the coil voltage and a significant plasma density increase depending on the total pressure.

Experimental Setup

The vacuum chamber is already described by Küllig *et al.* [3]. The inductive discharge arrangement consists of a planar double spiral antenna (2.75 windings, 115 mm diameter, copper) and a quartz cylinder. The quartz cylinder separates the antenna from the vacuum in the plasma vessel and serves as dielectric barrier. Through a matching network the RF power is transferred to the center connection of the antenna by the RF power generator.

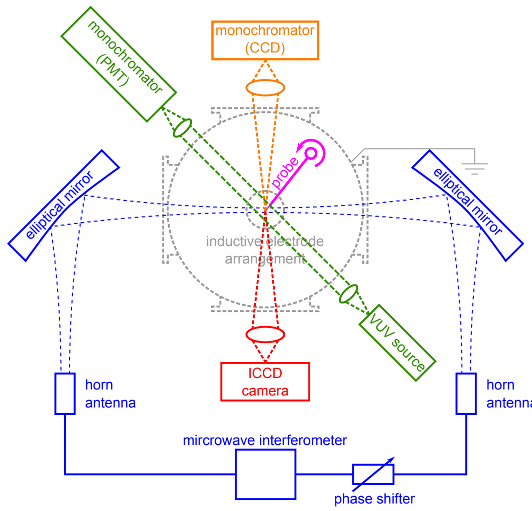

Figure 1: *Schematic top view picture of the experimental setup with the applied diagnotics.*

The process pressure is in the range between 5 and 35 Pa and the RF power was varried in the range from 1 to 600 W which leads to coil voltage between 1 and 8 kV. For some measurements the RF discharge power is pulsed with a frequency of 10 Hz and a duty cycle of 50 %.

Diagnostics

The Langmuir probe system (total length 150 mm) consists of a cylindrical platinum tip with lenght of 8 mm and diameter of 250 μm. The probe is passively compensated and the RF voltage is prevented by an additional filter unit. The Langmuir probe is axially and radially movable. Therewith, the entire plasma volume can be diagnosed. The positive ion saturation current was measured by biasing the probe sufficiently negative in respect to the floating potential. This allows an applicable degree of saturation. The electron temperature was determined by the inverse slope of the electron current.

The 160.28 GHz frequency stabilized (PLL) heterodyne mircowave interferometer measures non-invasive the phase shift between the propagating Gaussian beam through the plasma and a reference signal. Without any model assumption, this phase shift is proportional to the line integrated electron density. The microwave beam axis crosses the plasma in a distance of 30 mm from the bottom plate of the quartz cylinder. The Gaussian beam has a diameter of 10 mm in the discharge center. The time resolution amounts to 200 ns and the resolution of the line integrated electron density is about $5.3 \cdot 10^{13}\,\mathrm{m}^{-2}$.

The phase and space resolved optical emission at 844 nm was measured by means of a gated intensified charge coupled device (ICCD). The emission intensity patterns were radially averaged. The axially and temporally resolved excitation rate was calculated using the radially averaged emission intensity patterns together with the natural life time.

A monochromator was applied to measure the optical emission spectrum of the atmospheric A-band in the wavelength range of 749...778 nm. The PP and the PQ-branch were analysed to determine the rotational temperature from the inverse slope of the Boltzmann-Plot. For this investigated discharge the rotational temperature is comparable to the gas temperature.

Further, a monochromator for the VUV was adapted to determine the line inrtegrated density of the ground state and the metastables $\mathrm{O_2}\left(\mathrm{a}^1\Delta_\mathrm{g}\right)$ using the Lambert-Beer law. Therefore, the optical absorption in the wavelength range of 127...135 nm was measured. The ratio of the transmitted intensity to the intensity without absorbing gas/plasma is proportional to the gound state density and metastables density, respectively.

Results

Depending on the pressure the mode transition can be continuously or stepwise and changes the plasma parameter, electron heating mechanisms and electronegativity. At low RF power the E-mode is characterized by low positive ion saturation current and line integrated electron density at high electron temperature. With increasing pressure, the positive ion saturation current and line integrated electron density are lower and the transition starts at higher coil voltage. Additionally, the reduction of the coil voltage during the mode transition is higher for an increasing total gas pressure.

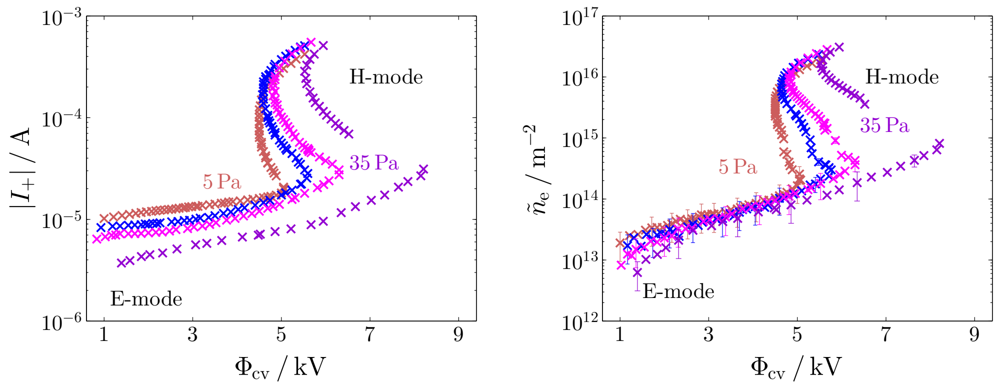

Figure 2: *Positive ion saturation current (left) and line integrated electron density (right) as function of coil-voltage for different total gas pressure of 5, 10, 15, 35 Pa.*

In the E-mode, the gas temperature is constant and comparable to room temperature (300 K). Further, the phase resolved optical emission reveals the electron heating due to the RF sheath heating during expansion and the electric field reversal during the sheath collapse [2]. The last one is an indication for high electronegativity [3]. With increasing the coil voltage the electrical field reversal vanishes and indicates a reduction of the electronegativity.

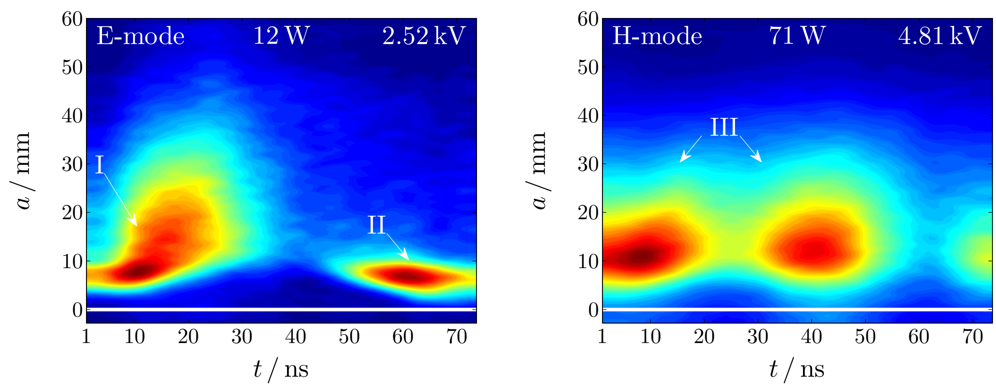

Figure 3: *Axially and phase resolved excitation rate patterns of atomic oxygen (844 nm) of an oxygen ICP in the E- and H-mode at a total pressure of 5 Pa.*

Addionally, the temporal behavior of the electron density in the early afterglow of a pulsed ICP was investigated. The line integrated electron density usually decreases in the afterglow due to recombination, ambipolar diffusion and wall losses. Nevertheless, a significant electron density peak appears in the early afterglow of the oxygen ICP. Without RF power the electron temperature and following the dissociative attachment reactions drop rapidly and lead to a lower production of negative ions. The density peak results from the collisional detachment of negative ions by metastable oxygen molecules [4]. The difference between the peak and steady state electron density represents a good measure for the negative ion density and the electronegativity of the oxygen discharge, respectively. These measurements confirm the high electronegativity in the E-mode.

The line integrated density of the metastables, $O_2\left(a^1\Delta_g\right)$, in the E-mode amounts to about 2% of the ground state density. With increasing RF power the discharge changes into the H-mode, which is characterized by high positive ion saturation current and line integrated electron density at lower electron temperature. The gas temperature is two times higher. During the mode transition the heating mechanisms change into two heating phases within one RF cycle. Further, the electronegativity in the H-mode is reduced. The line integrated density of metastables increases up to 6% of the ground state density.

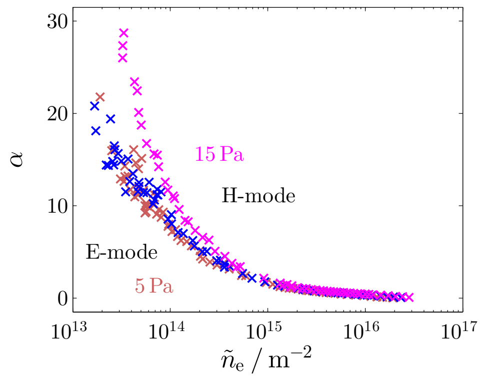

Figure 4: *Electronegativity as function of the line integrated electron density for different total gas pressure of 5, 15 Pa.*

Summary

The E- to H-mode transition of an oxygen ICP was studied in detail by comprehensive plasma diagnostics. It could be shown, that the mode transition changes the plasma parameter, electron heating mechanisms and electronegativity.

This work was supported by Deutsche Forschungsgemeinschaft, SFB TR 24.

References

[1] J. Hopwood, Plasma Sources Sci. Technol. **1**, 109 (1992)

[2] K. Dittmann, C. Küllig and J. Meichsner, Plasma Phys. Control. Fusion **54**, 124038 (2012)

[3] C. Küllig, K. Dittmann and J. Meichsner, Plasma Sources Sci. Technol. **19**, 065011 (2010)

[4] A Brockhaus et al., Plasma Sources Sci. Technol. **15**, 171 (2006)